Available online at www.sciencedirect.com
SCIENCE DIRECT®
Applied Catalysis B: Environmental 41 (2003) 371–386
APPLIED CATALYSIS B: ENVIRONMENTAL
www.elsevier.com/locate/apcatb

Photoelectrocatalytic and photocatalytic disinfection of *E. coli* suspensions by titanium dioxide

P.A. Christensen [a], T.P. Curtis [b], T.A. Egerton [a,*], S.A.M. Kosa [a], J.R. Tinlin [a]

[a] *Department of Chemistry, Bedson Building, The University of Newcastle upon Tyne, Newcastle NE1 7RU, UK*
[b] *Department of Civil Engineering, The Cassie Building, The University of Newcastle upon Tyne, Newcastle NE1 7RU, UK*

Received 18 March 2002; received in revised form 26 July 2002; accepted 26 July 2002

Abstract

This paper reports studies of the photoelectrocatalytic and photocatalytic disinfection of *E. coli* suspensions by titanium dioxide in a sparged photoelectrochemical reactor.

Two types of titanium dioxide electrode have been used. 'Thermal' electrodes were made by oxidation of titanium metal mesh; 'sol–gel' electrodes were made by depositing and then heating a layer of titania gel on titanium mesh. Cyclic voltammetry was used to carry out an initial characterisation and optimisation of both electrode types. The best 'thermal electrodes'—i.e. those with the highest photocurrents—were prepared by heating titanium mesh at ∼700 °C in air. For sol–gel derived electrodes, optimum performance was obtained by heating at ∼600 °C. These electrodes were then used, in a gas sparged reactor, to disinfect *E. coli* suspensions with an initial concentration of 10^7 colony forming units (cfu) ml^{-1}. Films prepared by the oxidation of titanium metal were shown to be superior to sol–gel derived films. Direct experimental comparison demonstrates that the photoelectrochemical system is more efficient than photocatalytic disinfection effected by slurries of Degussa P25 titanium dioxide.

Since in practical systems the TiO_2 would be exposed to a variety of species additional to those that are targeted, we also examined the effects of $H_2PO_4^-$ and HCO_3^- ions on the measured disinfection rates. Phosphate addition poisons both the electrode and particulate-slurry systems and is only partially reversible. By contrast, although bicarbonate addition affects all three systems, the effects are reversible.

Keywords: Photoelectrocatalytic and photocatalytic disinfection; Thermal electrodes; Sol–gel electrodes; Titanium dioxide (TiO_2)

1. Introduction

Photocatalytic oxidation by titanium dioxide has been extensively studied [1–3] and there is general agreement that the initial step is the UV excitation of electrons from the valence band to the conduction band of the titanium dioxide, followed by the formation of hydroxyl radicals. Recently, following the early work of Matsunaga et al. [4], photocatalytic destruction of bacteria by TiO_2 has merited increasing scientific attention [5–12]. Work on the interaction between *E. coli* inactivation and dihydroxybenzene isomers in the TiO_2 photocatalysed treatment of drinking water has been reported by Pulgarin and co-workers [10] and integrated photocatalytic-biological flow systems using supported TiO_2 and fixed bacteria for the treatment of biorecalcitrant herbicides have also been reported by these workers [11,12]. Particular advantages associated with this photocatalytic disinfection are that

* Corresponding author. Fax: +44-191-222-6929.
E-mail address: t.a.egerton@ncl.ac.uk (T.A. Egerton).

0926-3373/02/$ – see front matter © 2002 Elsevier Science B.V. All rights reserved.
PII: S0926-3373(02)00172-8

chlorine, a widely used treatment, does not destroy all pathogens and may itself give toxic by-products.

One major barrier to the technological development of photocatalytic oxidation and disinfection by TiO_2 has been the relatively low efficiency of light utilisation [13,14]. Low efficiency can arise because of both: (a) practical effects such as UV attenuation by the targeted liquid or fouling of reactor windows, and (b) intrinsic effects associated with low photocatalytic activity. A second barrier has been the need for post-treatment removal of TiO_2 from aqueous slurries of treated effluent.

Many authors [15–17] have reported that the initial disinfection rates depend on light intensity—a linear dependence on I is frequently reported in disinfection studies, even though electron–hole recombination would lead to an $I^{0.5}$ dependence of the intrinsic catalytic efficiency [14]. Because disinfection depends on light intensity, absorption and scattering of light by suspended TiO_2 particles may cause the disinfection rate to decrease if the TiO_2 concentration exceeds some critical value—as reported by Choi and Kim [18]. UV attenuation by window fouling can be minimised by reactor design, e.g. by ensuring turbulent flow. However, for a given reactor configuration, turbulence requires high flow rates and this reinforces the need for high intrinsic catalyst activity if efficient disinfection is to be achieved.

High intrinsic catalyst activity requires minimal recombination of UV generated charge carriers [14]. In principal this can be achieved by reducing, to significantly less than 100 nm, the migration distance over which the free charge carriers must travel [19]. However, in conventional photocatalytic treatment (in which the TiO_2 particles are dispersed as a slurry in the water to be treated) such small particles aggravate the difficulties of post-treatment separation of the photocatalyst. At the other end of the particle size spectrum, the flocculation induced by the inorganic aluminium and/or iron salts conventionally used for water treatment may result in catalyst sedimentation and consequent reduction in practical activity [16]. Both these drawbacks of slurry reactors have been addressed by immobilisation of catalyst on a fixed surface [15,18] but this introduces a new challenge—maintenance of good mass transfer of reactants to the catalyst surface.

A potentially promising route to improve intrinsic photocatalytic efficiency is to separate, and hence reduce the recombination of, the UV generated carriers by the use of an applied field—as represented schematically in Fig. 1. We have reported successful preliminary studies using this approach [20,21]. Photoelectrochemical disinfection of not only *E. coli* but also *Clostridium perfringens* spores [20] and *Cryptospiridium parvum* [21] was demonstrated. In our earlier studies of *E. coli* disinfection [22], the water to

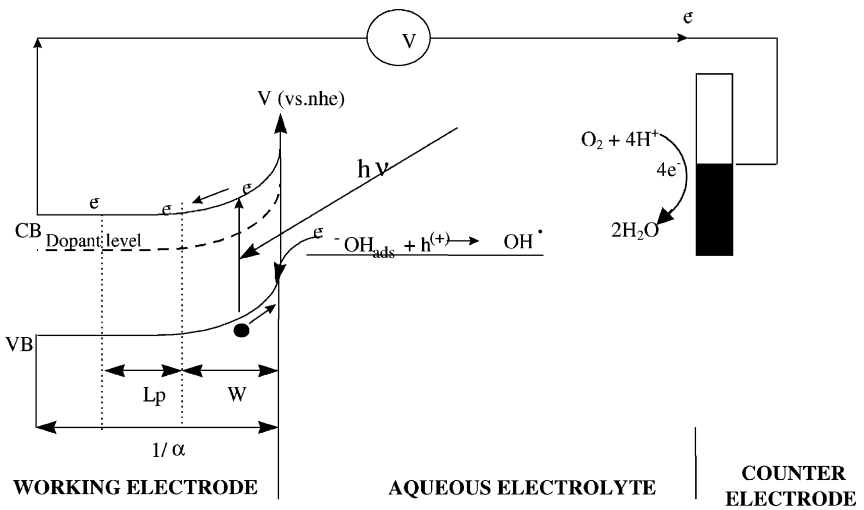

Fig. 1. An energy diagram showing the principal of the enhanced photo-activity that results from the reduced recombination of charge carriers associated with an applied electrical field, where L_p is the minority carrier length, W the depletion layer width, α the absorption coefficient, and $1/\alpha$ is the penetration depth of light.

be disinfected was irradiated from above using two 8 W UVA lamps. Comparison of photoelectrochemical with published (by others) photochemical disinfection rates suggested that the rate of photoelectrochemical disinfection at TiO_2 electrodes rate was superior to photo-disinfection by particulate slurries; however, differences in lamps and variations of electrode surface area introduce considerable uncertainties into quantitative comparisons of this type.

In separate studies, Harper et al. have developed a reactor that seeks to minimise the consequences of strongly absorbing/scattering liquids [23]. A concentric electrode assembly is placed around an axially mounted UV lamp. To minimise the UV attenuation the UV path length is reduced to ∼2 mm. Potential mass transfer problems resulting from this approach are minimised by using mesh electrodes and by sparging the reactor with a stream of gas. In this way we achieved the turbulence necessary to promote mass transfer and to minimise window fouling.

In this paper we report the use of such a reactor for the photoelectrochemical disinfection of water inoculated with *E. coli*. We have examined the performance of two different electrode systems and related their properties to their electrochemical characteristics measured by cyclic voltammetry. We have also directly compared the photoelectrochemical system with photocatalytic disinfection by slurries of P25 high area titanium dioxide. Finally, since electrodes in real water systems are exposed to a variety of species additional to those that are targeted, we compared the sensitivity to HCO_3^-, a radical scavenger, and $H_2PO_4^-$, a potential poison, of the two TiO_2 photo-anodes and the particulate TiO_2 photocatalyst.

2. Experimental

2.1. The photoelectrochemical reactor

The photoelectrochemical reactor is shown in Fig. 2 and was only half the height (with one, not two, electrode cassettes) but otherwise similar to that previously described [23]. The reaction volume is enclosed

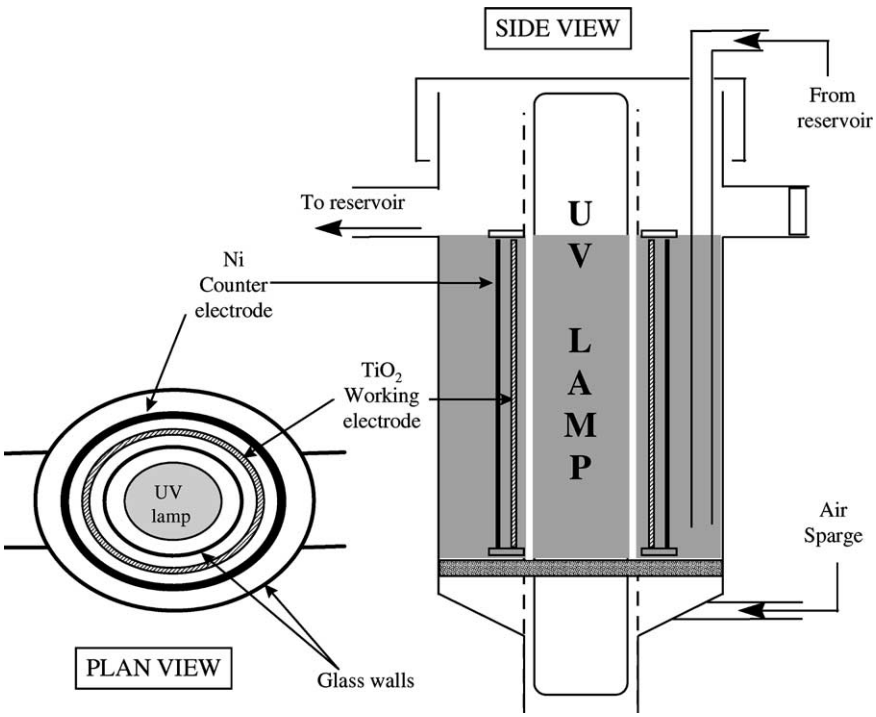

Fig. 2. Plan and elevation of the photoelectrochemical reactor, showing the UV lamp positioned axially within a concentric TiO_2 anode and a nickel mesh counter electrode. The 0.5 dm^3 reactor was operated by itself or connected in a re-circulation loop to a 2 dm^3 reservoir.

between a vertical inner Pyrex glass tube (42 mm external diameter) and an outer concentric (80 mm i.d.) tube. A sintered frit placed horizontally at the bottom of the reactor acts as a distributor for the sparge gas. The tubular UV source (two 8 W Black Lamp, Philips) is located within the inner annulus along the axis of the reactor. Within the reaction volume is an electrode cassette composed of a cylindrical (100 mm long × 22 mm radius) TiO_2 diamond mesh (42% open area with 1.5 mm × 1 mm holes) electrodes separated by 2 mm Teflon spacers from the nickel mesh counter electrodes. Prior to experiments the reactor was sterilised by autoclaving at 121 °C for 20 min and during operation was enclosed in an aluminium box.

2.2. Electrode fabrication and characterisation

2.2.1. Thermal electrodes

The thermal electrodes were fabricated by heating a cylinder of titanium metal mesh for 10 min in a horizontally mounted tube furnace, preheated to the designated temperature. The oxidised cylinders were then removed from the furnace and allowed to cool naturally in air. As described later, the performance of these electrodes depended on the treatment temperature. The characterisation experiments described in Section 2.3 identified a maximum in the UV induced photocurrent at treatment temperatures in the range 700–750 °C. Therefore, except where otherwise specified, a standard treatment temperature of 700 °C was used.

2.2.2. Sol–gel electrodes

Sol–gel electrodes were fabricated by depositing a layer of titania gel on the titanium metal mesh cylinders prior to heat treatment. The titania gel was made by hydrolysing titanium isopropoxide in water acidified with nitric acid, as described by O'Regan et al. [24]. The resulting sol was then concentrated to ca. 150 g l^{-1}; during this stage the viscosity of the fluid increased, indicating the formation of a gel network. The electrodes were dipped in the gel, drained and then spun about a horizontal axis at 2800 rpm. The coated assembly was then heated for 10 min in the tubular furnace used for thermal electrodes—again the electrode performance depends on the treatment temperature. On the basis of the cyclic voltammetry characterisation (Section 2.3) a standard heat treatment at 600 °C was chosen. The heated films had a thickness of ca. 2–5 μm.

2.3. Electrode characterisation

Electrochemical characterisation of thermal electrodes was carried out on 5 cm × 5 cm × 0.3 cm titanium plate electrodes (Goodfellow 99.6%) prepared in a manner that closely replicated the treatment of the mesh electrodes. Sol–gel test-electrodes were prepared by dropping the gel solution onto 1 cm × 1 cm plates which were then spun at 2800 rpm prior to heating. Characterisation of the electrodes was then carried out by cyclic voltammetry, with a sweep rate of 100 mV s^{-1}, using a Sycopel AEW2 potentiostat. Potentials are quoted relative to in-house Ag/AgCl reference electrodes, calibrated against a commercial (Sentek) reference electrode. Powder X-ray diffractograms were measured using a Philips diffractometer using nickel filtered Cu Kα radiation.

2.4. Disinfection experiments

2.4.1. E. coli sample preparation

E. coli ((NCIMB 8277) were grown overnight at 37 °C in nutrient broth (Oxoid, UK) on a rotary shaker (@150 rpm). The 5 cm^3 aliquots were centrifuged at 3000 rpm for 10 min, washed twice in sterile Milli-Q water and re-suspended in 5 cm^3 of Milli-Q water.

2.4.2. Reactor operation

De-ionized water, rendered conductive by the addition of 200 mg l^{-1} of Na_2SO_4, was inoculated with *E. coli* to give an initial concentration of $\sim 10^7$ colony forming units (cfu) ml^{-1}. This water was chosen because in preliminary measurements, using tap water, variable disinfection rates caused by variations in the chlorine content of the laboratory water supply were measured. Electrochemical control and measurement was by a Sycopel AEW2 potentiostat and potentials are quoted relative to the nickel gauze counter electrode (the reactor was operated in two-electrode mode, without a reference electrode). The reactor was then illuminated, by two 8 W UVA lamps (Philips Lighting UK model TL/02/08), and operated with a flow of N_2 sparge gas. During operation, the progress of disinfection was monitored by sampling the reactor contents at 5 min intervals and the bacteria counted as described

later. Each experiment was repeated at least twice and in Fig. 5b the results of three independent replicate experiments illustrate the degree of reproducibility obtained. However, for the sake of clarity, the remaining figures show the results of a single experiment (i.e. without averaging the results of replicates).

2.4.3. *E. coli* analysis

To determine the concentration of bacteria, the tested suspensions were diluted to a suitable concentration with Ringers solution and then spread uniformly on to nutrient agar (Oxoid, UK) plate. After an overnight incubation at 37 °C, the colonies were counted and the initial number of bacteria was calculated. In all counts at least three replicate plates were used and the results were reproducible within an average relative error of 10%. (Bacterial colonies counts were usually between 30 and 300, fewer than 30 are inaccurate because a single contamination can cause at least 4% error and over 300 are difficult to count.) Although, for clarity, error bars have not been routinely included in the figures, a typical spread is shown in Fig 5b.

3. Results

3.1. Electrode characterisation

The current–voltage curves of both the thermal and sol–gel electrodes, measured on the small test-electrodes, are shown in Fig. 3A and B measured in either tap water or methanol before and during UV irradiation. For the thermal oxide film, a plot of the photocurrent versus the square root of $(V - V_{onset})$ where V_{onset} is the potential at which an anodic photocurrent is first observed, is approximately linear, as predicted by classical semiconductor theory [25]. By contrast, the current–voltage curve of the sol–gel electrode does not appear to follow classical theory, as the photocurrent appears to be almost independent of the applied potential between 0 and 1.2 V versus Ag/AgCl. Vinodgopal et al. [26] has suggested that this behaviour is consistent with the fact that, in very small undoped particles, the electric field across each particle would be insufficient to facilitate charge separation. Under these circumstances, it is more reasonable to consider that the increased efficiency reported below results from different rates of charge-carrier transport across the whole film rather than across the individual component particles of the film.

Further information on the electrode performance was then obtained by measuring current–voltage curves in a solution of methanol, which is known to capture holes effectively [27]. For the thermal films, the current–voltage curves (Fig. 3A) are not affected by the addition of methanol and this suggests that photo-generated holes which reach the surface are captured effectively by surface hydroxyl groups. For the sol–gel films, by contrast, addition of methanol causes a three-fold increase in the photocurrent at 0.5 V. Fujishima and co-workers [28] reported similar increases following the addition of ethanol to 0.2 M Na_2SO_4 solution and concluded that the alcohol addition had suppressed the recombination processes at the surface of their spray-pyrolysed TiO_2 photoelectrodes. Indeed from intensity modulated photocurrent spectroscopy results they concluded that on their electrodes alcohol addition resulted in virtual suppression of the entire process of charge transfer to surface states.

Fig. 4a and b summarises the variation in the photocurrent, measured on 1 cm × 1 cm electrodes, with increase in heating temperature for both thermal and sol–gel films and demonstrates that at temperatures ∼650 °C for sol–gel films or ∼750 °C for thermal films, there is a decrease in measured photocurrent. X-ray diffraction shows increasing amounts of rutile above these temperatures and scanning electron microscopy demonstrates that the surface becomes rougher—possibly associated with the change in density that accompanies rutile formation.

3.2. Disinfection experiments

3.2.1. Results for blank experiments

Under the conditions used in these experiments, UV irradiation did not, by itself, cause significant destruction of *E. coli* in the absence of an applied potential (Fig. 5a and b). Nor did the application of small positive potentials (1.2–3 V) to unirradiated electrodes cause significant disinfection. By contrast, Fig. 5a and b shows that significant disinfection occurred when a small potential was applied to UV-irradiated electrodes of either type.

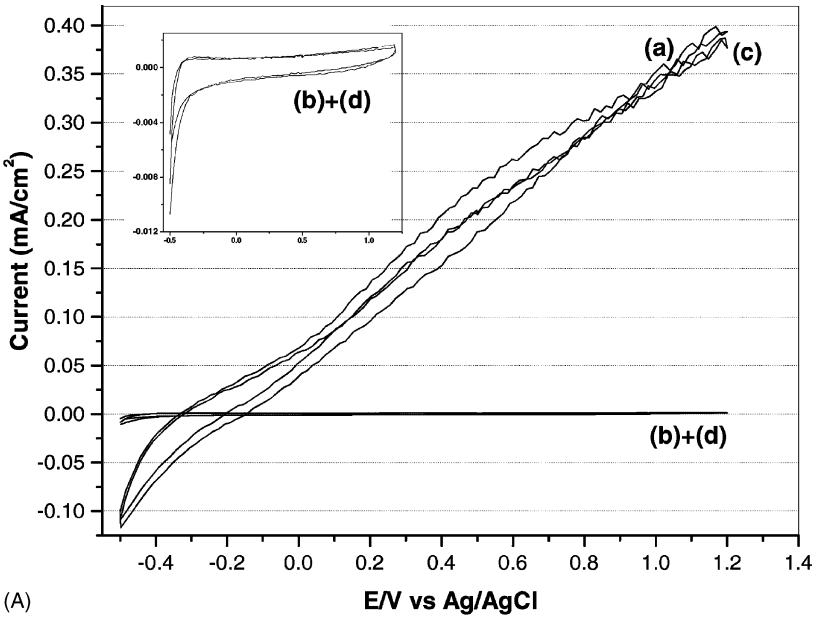

(A)

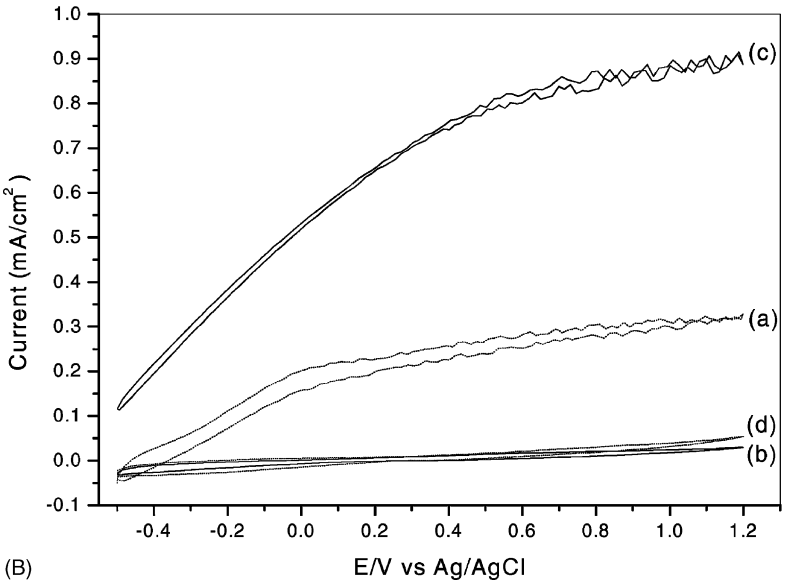

(B)

Fig. 3. (A) Cyclic voltammograms (100 mV s^{-1}) of thermal-film electrodes prepared by heating for 10 min at 700 °C, measured in tap water when: (a) UV-irradiated, and (b) in the dark; and in a 1 M solution of methanol in tap water (c) with UV irradiation, and (d) in the dark. (B) Cyclic voltammograms (100 mV s^{-1}) of the sol–gel electrodes, prepared by depositing and heating five layers of the TiO_2 suspension, measured in tap water when (a) UV-irradiated, and (b) in the dark; and in a 1 M solution of methanol in tap water with (c) UV irradiation, and (d) in the dark.

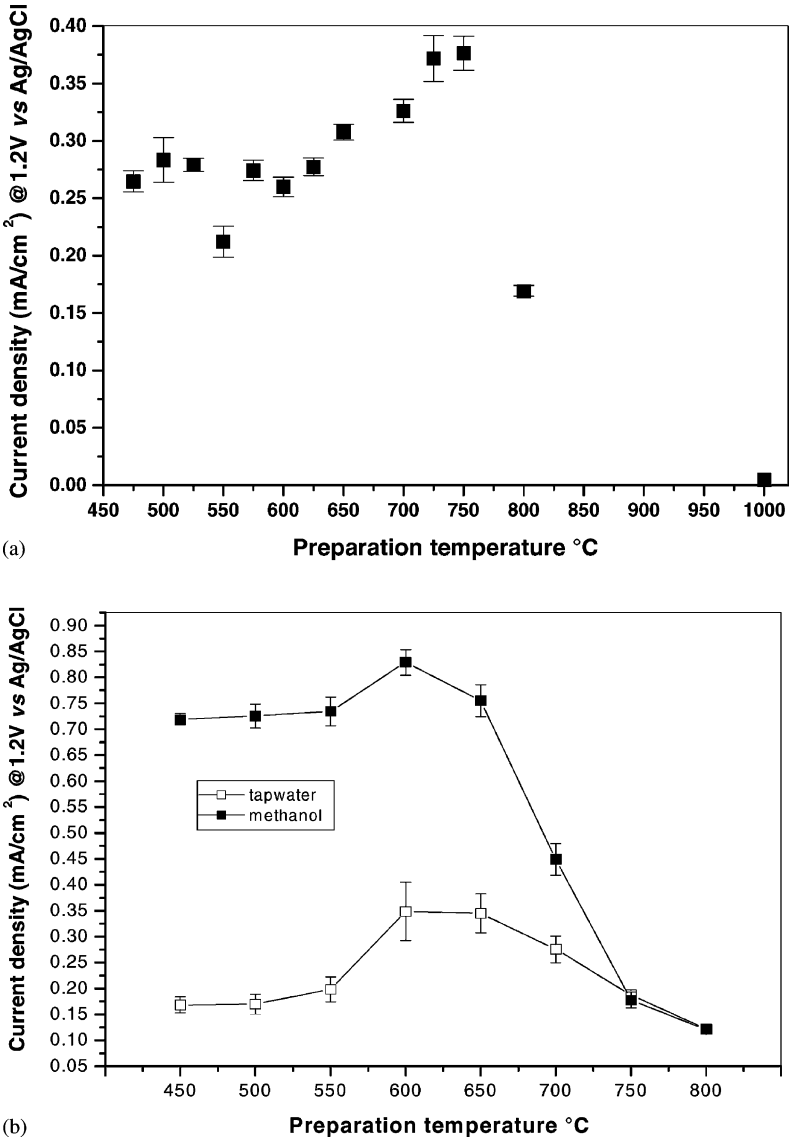

Fig. 4. (a) Current density at 1.2 V (vs. Ag/AgCl) as a function of fabrication temperature of thermal-film electrodes. The measurements are the mean of two replicate experiments. (b) Current density at 1.2 V (vs. Ag/AgCl) as a function of preparation temperature of sol–gel electrodes prepared by five successive coatings from a suspension of 147 g TiO_2 dm^{-3}. In tap water (□), and in a 1 M solution of methanol in tap water (■). Each experimental point is the mean of two replicate experiments.

3.2.2. Results for sol–gel electrodes

Fig. 5b shows the results of disinfection experiments with sol–gel electrodes prepared at 600 °C. In each case, 0.5 dm^3 of water was injected with *E. coli* to give an initial concentration of ~10^7 colony forming units ml^{-1}. The results of three separate experiments at a potential of 3.0 V, relative to the nickel counter electrode, demonstrate the reproducibility achieved. In this study, no attempt to derive detailed kinetics was made; however, a simple analysis showed that the order is less than one and this is consistent with the value of 0.43 determined for sol–gel electrodes

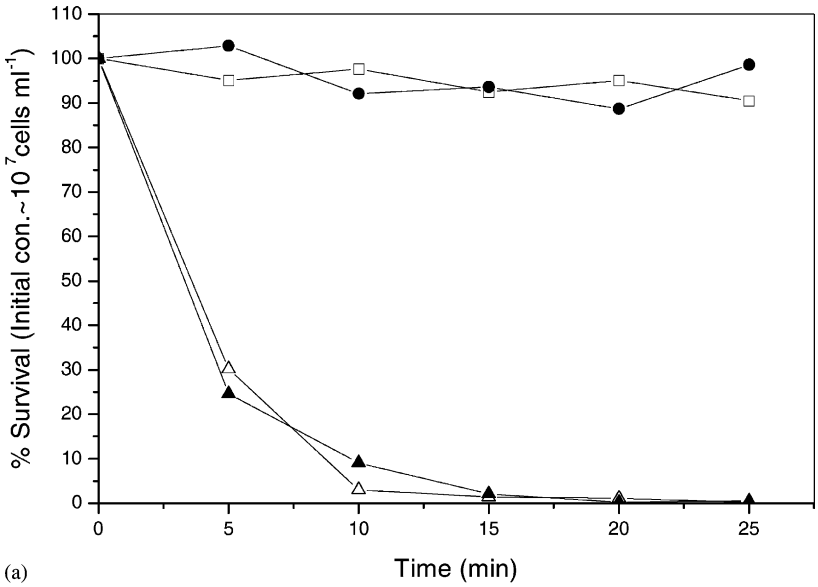

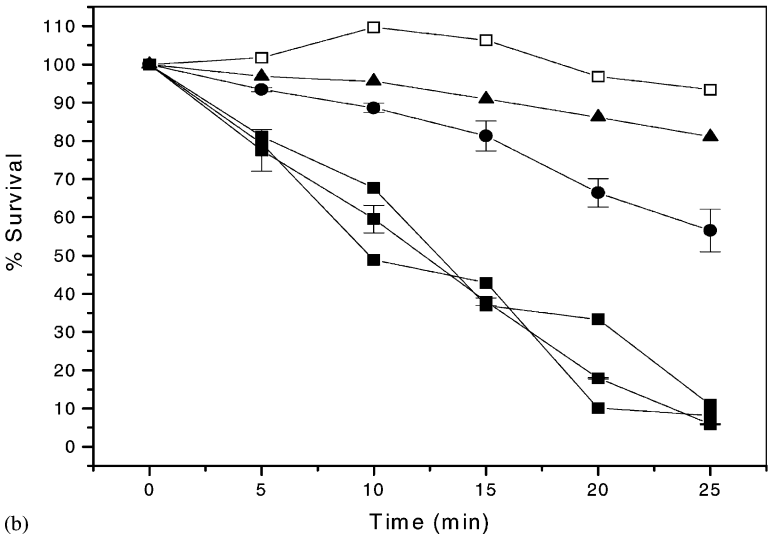

Fig. 5. Comparison of *E. coli* destruction by UV light (only) and by the thermal and sol–gel electrode: (a) UV-irradiated gas sparged either with a thermal electrode in place but no applied potential, or without an electrode in place (□); thermal electrode at a potential of 1.3 V, gas sparged in the dark (●); thermal electrode at a potential of 1.3 V, UV-irradiated and gas sparged (△), thermal electrode at a potential of 3.0 V, UV-irradiated and gas sparged (▲). The initial concentration of *E. coli* was 4.6×10^6 cfu.
(b) UV-irradiated gas sparged only (□); UV-irradiated gas sparged with sol–gel electrode in place but no applied potential (▲); sol–gel electrode at a potential of 1.3 V, UV-irradiated and gas sparged (●); sol–gel electrode at a potential of 3.0 V, three separate experiments shown to demonstrate reproducibility (■). The initial concentration of *E. coli* was 7.6×10^6 cfu.

in our earlier study [22]. At 3 V, 95% of the initial concentration of *E. coli* was destroyed in 25 min and 35% in 10 min. At 1.2 V, only 15% of the bacteria were killed after 10 min irradiation of the sol–gel electrode.

3.2.3. Disinfection by thermal-film electrodes and the effect of fabrication temperature

The corresponding results for a thermal electrode is shown in Fig. 5a from which it is immediately obvious that the thermal electrode is significantly more effective than the sol–gel electrode, at killing *E. coli*. Even with an applied potential of only 1.3 V, more than ~95% of the bacteria were killed in 10 min, much more than the 15% destroyed with the sol–gel electrode at the same potential. A simple analysis suggests approximately first-order kinetics, consistent with the results of our earlier more detailed kinetic study of thermal electrodes [22]. Because no further improvement in activity resulted from increasing the applied potential from 1.3 to 3.0 V, a standard potential of 1.3 V was used in subsequent experiments with thermal electrodes. Fig. 6 shows that the performance of these electrodes broadly mirrors the pattern implied by the photocurrent measurements shown in Fig. 4b. The optimum disinfection rate was obtained with thermal electrodes that had been heated to 700 °C, cf. maximum photocurrent at 725–750 °C, and an increase in fabrication temperature to 800 °C was sufficient to reduce the disinfection rate very significantly.

It may be noted that even though the thermal film is a more active photoelectrocatalyst than the sol–gel film, it is a less active photocatalyst, i.e. in the absence of an applied potential the sol–gel electrode is more active. An understanding of this difference requires further characterisation of the two electrode types.

3.2.4. Results for disinfection of large volumes by sol–gel and thermal films

For both thermal and sol–gel electrodes additional experiments were conducted in which an external 2 dm^3 reservoir was connected to the reactor by a peristaltic pump and the reactor was then operated in a recycling mode at a flow rate of 100 ml min^{-1}. These results are shown in Fig. 7 and confirm the superiority of the thermal electrodes but demonstrate that even with the less efficient sol–gel electrodes, at 3 V, over 95% disinfection was achieved in 80 min. The corresponding disinfection was achieved in 20 min for the

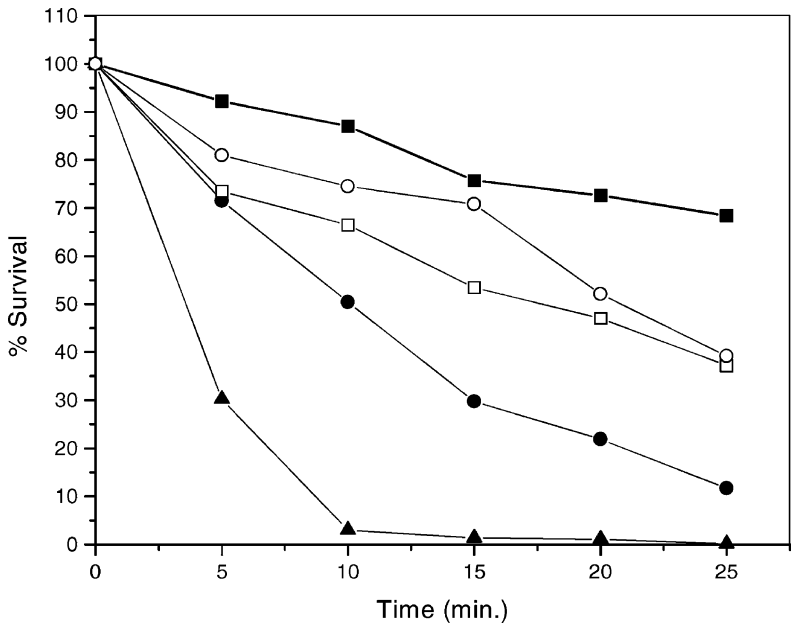

Fig. 6. Destruction of *E. coli* (initial concentration 6.2×10^6 cfu) by UV-irradiated thermal films fabricated at increasing temperatures (450 °C (○), 600 °C (●), 700 °C (▲), 750 °C (□), 800 °C (■)). The maximum rate was obtained for electrodes heated to 700 °C.

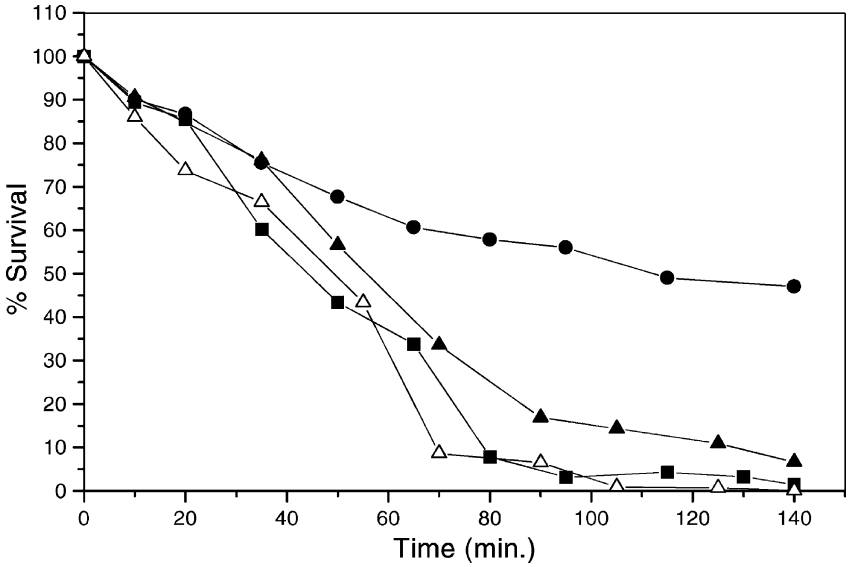

Fig. 7. A comparison of the efficacy of thermal (at 1.3 V (▲), 3.0 V (△)) and sol–gel electrodes (at 1.3 V (●), 3.0 V (■)) for the destruction of *E. coli* (initial concentration 1.25×10^7 cfu). These measurements were made by recirculating 2.5 dm^3 of *E. coli* inoculated water through the reactor. The time for 50% kill is approximately 5× that for the sparged 0.5 dm^3 reactor.

0.5 dm^3 capacity of the reactor in the absence of the external reservoir. Hence, in these exploratory studies any affects of bypassing appear to be negligible.

3.2.5. Effect of light intensity (I)

Simple studies of the effect of light intensity were carried out by comparing disinfection rates with either one or two axially mounted lamps. For the thermal electrodes, the first-order rate plots (Fig. 8) suggest that replacing one lamp by two doubles the rate, and implies I^1 intensity dependence. For the sol–gel electrodes, doubling the light intensity increased the disinfection from ∼40 to ∼60%, and we cannot differentiate between $I^{0.5}$ and I^1.

3.2.6. Comparison of disinfection by electrodes and TiO_2 slurry

A key question is whether photoelectrochemical disinfection is more efficient than photocatalytic. Although a number of comparisons have been made in the literature [22], these often rely on assumptions about the relative areas of active surface, etc. Therefore, we have carried out a direct comparison in which the electrode assembly was removed from the reactor and replaced by a slurry of Degussa P25 titania as the active catalyst. A TiO_2 concentration of 8 g dm^{-3} was used since studies by us of isopropanol oxidation as a function of TiO_2 level had shown that maximum activity was reached by this slurry. Other conditions such as *E. coli* concentration, UV sources and gas sparge rates were kept constant. The results shown in Fig. 9 demonstrate that for both electrode systems the rates of photoelectrochemical disinfection significantly exceed the rate of photocatalytic disinfection by Degussa P25.

3.2.7. Effect of interfering species

Practical disinfection systems must be sufficiently robust to maintain their activity in the presence of adventitious poisons and radical scavengers. Therefore, we have investigated the resistance of all three systems to potassium hydrogen phosphate and sodium bicarbonate.

Phosphate is known to adsorb strongly on titanium dioxide surfaces perhaps by an exchange reaction between surface hydroxyl groups and $H_2PO_4^-$ ions [29]. The adsorption is so strong that it inhibits the anatase–rutile transformation that can otherwise be induced by milling Degussa P25 [30]. Matthews and co-workers have demonstrated that phosphate

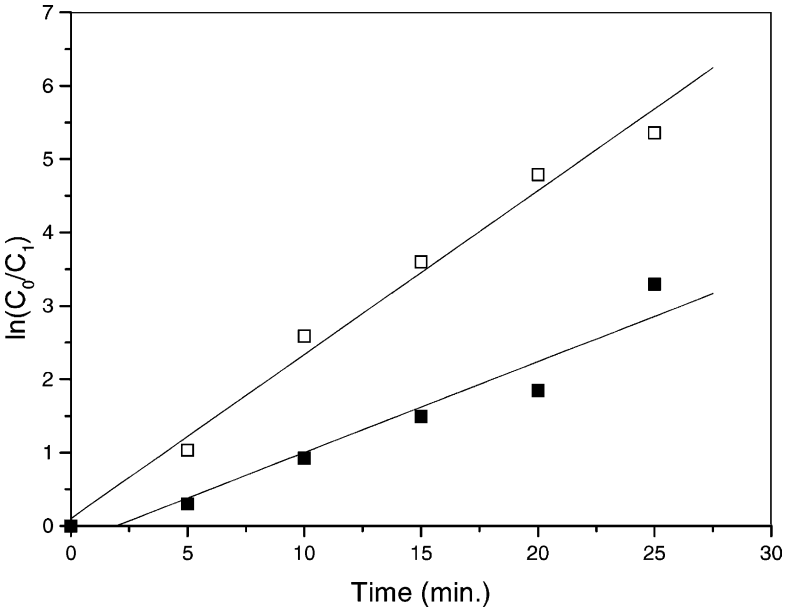

Fig. 8. The effect of light intensity for one UV lamp (■), and two UV lamps (□) for a thermal film at a potential of 1.3 V vs. nickel counter electrode.

adsorption at concentration as low as 1 mM reduces photo-oxidation of simple organics (ethanol, aniline and salicylic acid) by ∼50% [31]. We have therefore investigated the effect of phosphate addition on the disinfection efficiency of both the electrodes and the P25. Fig. 10 shows detailed results for thermal films and demonstrates that phosphate decreased in the effectiveness of all three TiO_2 systems. A 4 mM

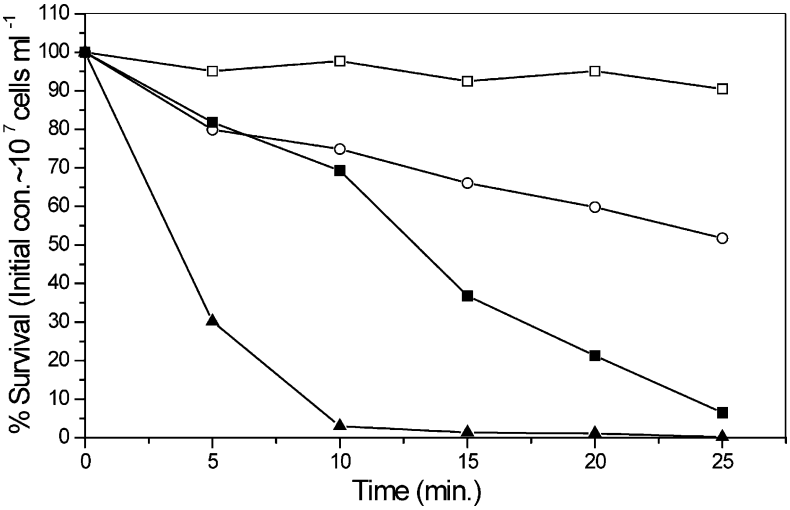

Fig. 9. A comparison of photoelectrochemical destruction of *E. coli* (initial concentration 5.1×10^6 cfu) with photocatalytic destruction by a slurry of P25. UV light (only) (□), sol–gel electrode at 3.0 V (■), thermal electrode at 1.3 V (▲), and operation of the reactor in slurry mode with 8 g TiO_2 dm^{-3} (○).

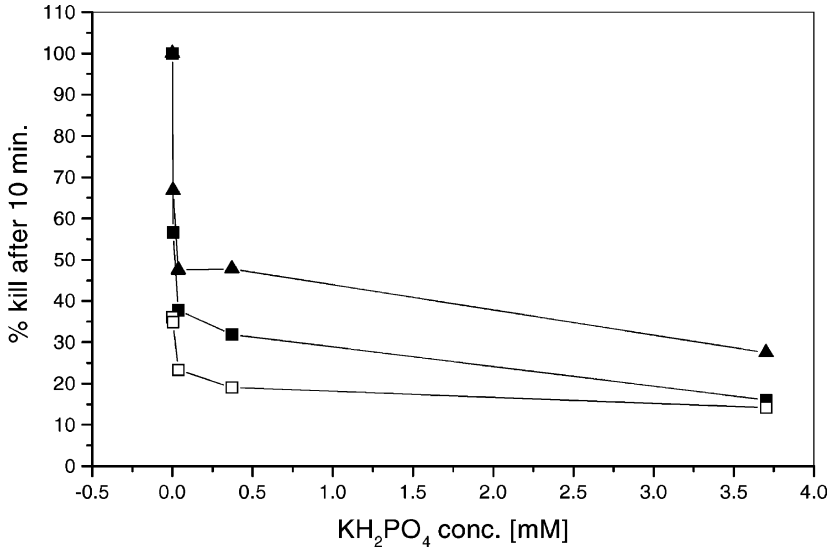

Fig. 10. The percentage decrease in disinfection ability associated with increasing concentrations of phosphate. Results for thermal electrodes (■), for operation of the reactor in slurry mode (□), and for the thermal electrodes exposed to phosphate and then washed with cold tap water and subsequently rinsed in distilled water (▲). The initial concentration of *E. coli* was 2.7×10^6 cfu.

solution of K_2HPO_4 decreased the '10-min kill' of both the electrodes and of the particulate slurry to a similar value, $15 \pm 2\%$. The binding of the $H_2PO_4^-$ ions on the surface of the TiO_2 was sufficiently strong that the disinfection activity was only partially restored by washing the electrode with copious quantities of tap water (Fig. 10), or by 5 M sulphuric acid at 100 °C. Even reheating the electrodes for 10 min at 700 °C failed to regenerate the catalytic activity.

Carbon dioxide dissolved in water is in equilibrium with HCO_3^- and CO_3^{2-} (and an analysis of typical tap water in our laboratory shows a bicarbonate content of 22 mg l^{-1}). Both of these ions can, by competitive reaction with $OH^\bullet$, poison the photocatalytic activity of titanium dioxide. The disinfection rate by thermal electrodes in the presence of bicarbonate is shown in Fig. 11a, whilst Fig. 11b shows the effect of bicarbonate on both the two electrode systems and the slurry reactor. Fig. 11b shows for both electrochemical and photochemical operation, addition of bicarbonate decreases the disinfection efficiency. In 100 mg dm^{-3} (1.2 mM) solutions of sodium bicarbonate, the percentage of *E. coli* destroyed in 10 min was reduced from 100 to 30% for the thermal film, from 40 to 17% for the sol–gel electrode and from 37 to 6% for the particulate slurry. For the electrodes, the residual activity is about 1/3 of the activity in bicarbonate-free water whereas the activity of the bicarbonate additioned slurry is only 1/6 of that in bicarbonate-free water. However, it is important to note that the effect of the bicarbonate is reversible. Fig. 12 shows that the catalytic activity of the thermal electrode was re-established by washing it with warm distilled water.

4. Discussion

The points for discussion fall into three main areas: (a) the practical effectiveness of electric field enhancement at titanium dioxide photo-anodes; (b) the consequences of the different methods of anode fabrication; (c) an analysis of the reasons for these differences, in order to design improved systems.

4.1. The effectiveness of electric field enhancement

The results confirm earlier demonstrations, from relatively small-scale experiments, that the application of very modest potentials to titanium dioxide surfaces enhances disinfection rates and extends the concept to

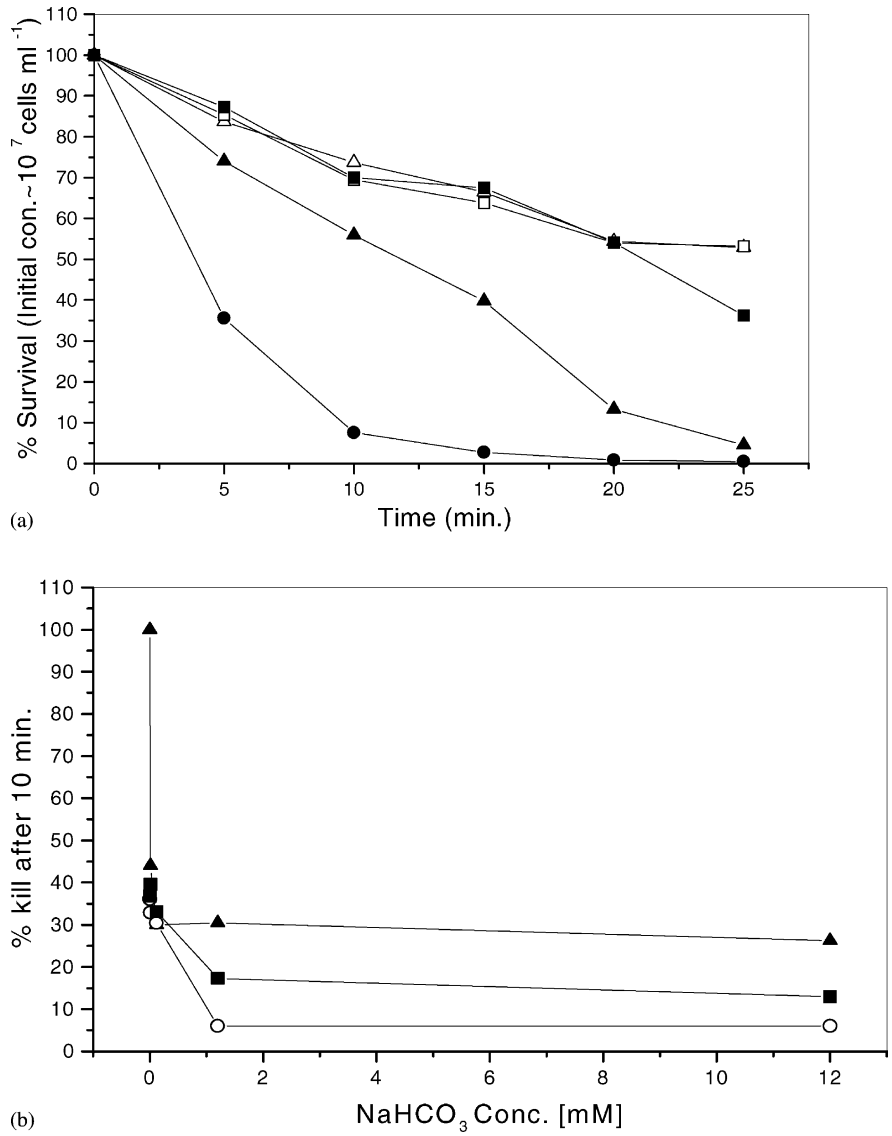

Fig. 11. (a) The reduction in disinfection rate for thermal electrodes in the presence of bicarbonate (added as sodium bicarbonate with no attempt to control the pH). Results without $NaHCO_3$ dm^{-3} (●), and with 1 mg $NaHCO_3$ dm^{-3} (▲), 10 mg $NaHCO_3$ dm^{-3} (■), 100 mg $NaHCO_3$ dm^{-3} (□), and 1000 mg $NaHCO_3$ dm^{-3} (△). The initial concentration of *E. coli* was 2.2×10^7 cfu. (b) A comparison of the effect of bicarbonate on the rate of *E. coli* destruction at increasing concentrations of bicarbonate. Results for thermal (▲), and sol–gel (■) electrodes, and for operation of the reactor in slurry mode (○). The initial concentration of *E. coli* was 6.8×10^6 cfu.

reactors capable of scale-up. Larger reactors can be achieved simply by increasing the number of electrode cassettes.

We have, for the first time, directly compared the efficiency of the photoelectrocatalytic process with that of direct photocatalytic disinfection and have demonstrated that, despite the small geometric area of the electrodes (~100 cm^2 illuminated per cassette), photoelectrocatalytic disinfection is more effective than direct photocatalytic disinfection by particulate Degussa P25, the standard particulate photocatalyst, with a surface area of 50 m^2 g^{-1}. Further, despite their

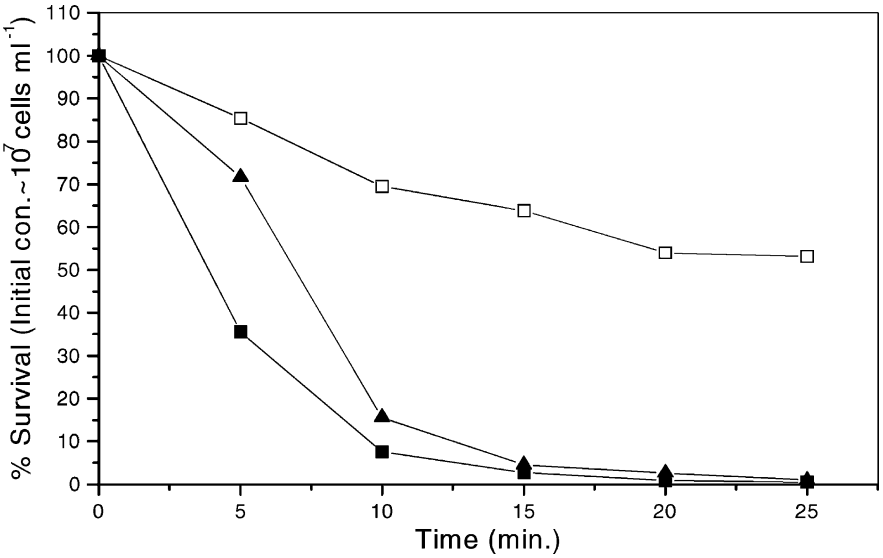

Fig. 12. Disinfection rate curves for thermal electrodes showing the reversibility of the effects of bicarbonate. Initial results for thermal electrode without bicarbonate addition (■), after the addition of 100 mg $NaHCO_3/L$ (□), and after subsequent washing of the electrodes with cold tap and a subsequent rinse in distilled water (▲). The initial concentration of *E. coli* was 4.4×10^6 cfu.

relatively low surface area, these photo-anodes are less sensitive to poisoning by phosphate than the corresponding particulate system. In addition, we have shown that the electrode systems are less affected by bicarbonate, the species which has, because of its ubiquity, been the ion of most concern with respect to deactivation of titanium dioxide

Most significantly, our preliminary measurements suggest that the effectiveness of these electrodes increases as I^1 whereas, model photo-oxidation reactions suggest that because of electron–hole recombination, the efficiency of slurry reactors may only increase only as $I^{0.5}$. The photoelectrocatalytic system is therefore potentially more able to exploit the increased light intensities associated with, e.g. solar concentrators and this tentative conclusion will be examined further in future work.

4.2. Differences between electrodes

The thermal electrodes are clearly more efficient than the sol–gel electrodes for the destruction of *E. coli*. Studies of destruction of *C. parvum* spores have also shown that thermal films were more effective than sol–gel electrodes [21]. These differences are counter intuitive because sol–gel electrodes are thought to have a greater surface area than the thermal electrodes and could therefore be assumed to be more effective. Earlier small-scale experiments [22], also showed that the disinfection kinetics were first-order for thermal films and half-order for sol–gel films. Previous work [19] with a 30 cm disc reactor has suggested that sol–gel and anodic titanium oxide films behave similarly with respect to phenol degradation whilst recent, unpublished [32] work by us has shown that commercially supplied TiO_2-based electrodes are particularly effective for both oxalic acid and nitrophenol photo-oxidation. This specificity mirrors the conclusions from liquid phase photocatalytic studies that the activity-ranking of different commercial titanium dioxide catalysts depends on the reaction that is being studied [33], and implies that commercialisation of photoelectrocatalytic reactors may require the electrodes to be tailored to specific applications.

4.3. Reasons for differences in electrode performance

The greater effectiveness of the thermal over the sol–gel electrodes is paralleled by: (a) the greater

dependence of photocurrent on applied potential, and (b) the reduced sensitivity of measured photocurrent to the presence of methanol. These observations are consistent with more effective reduction of charge-carrier recombination in thermal films in which the application of a small potential allows the development of a depletion layer in which effective charge separation can occur. The depletion layer thickness, and consequently the photocurrent, increases, roughly, with the square root of the applied potential as was demonstrated in our earlier study [22]. At a fixed applied potential the number of charge carriers is predicted to be proportional to the light intensity if recombination has been suppressed (contrary to the $I^{0.5}$ relationship expected when recombination dominates). This is consistent with our present results, although work over a wider range of light intensity is necessary to test this point more fully.

In the work on sol–gel derived electrodes it is probable, as suggested by Vinodgopal et al. [26], that the particles are significantly smaller than the depletion layer thickness and for this reason are too small to show an appreciable potential drop across their width. The benefits of electric field enhancement are reduced since there is significant residual recombination of electrons and holes. We conclude that methanol increases the photocurrent because, as demonstrated for ethanol by Semenikhin et al. [28], alcohol addition suppresses recombination that would otherwise occur at surface states.

By contrast, because there is much less residual recombination of charge carriers at the surface of the thermal electrodes and any effect of methanol is negligible. In future work we will (a) seek additional information on the surface morphology, and (b) test this interpretation, and hence improve electrode efficiency by deliberately decreasing the depletion thickness/particle size ratio in sol–gel particles.

5. Conclusions

The results demonstrate that scale-up of photoelectrochemical disinfection by titanium dioxide is practical and show that robust electrodes prepared by thermal treatment of titanium mesh are more active than electrodes prepared by a sol–gel route.

We have shown by direct comparison, of measurements made in the same reactor, that both thermal and sol–gel electrodes are more active than a slurry of P25 particulate TiO_2. We have also shown that they are more resistant both to poisoning by $H_2PO_4^-$ and to the presence of HCO_3^- in solution.

Significantly increased rates can be achieved by increasing the intensity of UV irradiation (I), since disinfection rates increase as I^1. Our future work will focus on further improvement in electrode activity.

Acknowledgements

We thank the Cultural Bureau of the Royal Kingdom of Saudi Arabia for support for SAMK and the EPSRC for financial support of JRT.

References

[1] A. Mills, S. Le Hunte, J. Photochem. Photobiol. A 108 (1997) 1.
[2] A. Christensen, G.M. Walker, Opportunities for the UK in Solar Detoxification, ETSU s/P4/00249/REP, 1996.
[3] A. Fujishima, T.N. Rao, Pure Appl. Chem. 70 (1998) 2177.
[4] T. Matsunaga, R. Tomoda, T. Nakajima, H. Wake, Microbiol. Lett. 29 (1985) 211.
[5] M.R. Hoffmann, S.T. Martin, W. Choi, D.W. Bahnemann, Chem. Rev. 95 (1995) 69.
[6] M. Bekbolet, Water Sci. Technol. 35 (1997) 95.
[7] P.K.J. Robertson, L.A. Lawton, B. Münch, J. Ronzade, Chem. Commun. (1997) 393.
[8] K. Sunada, Y. Kikuchi, K. Hashimoto, et al., Environ. Sci. Technol. 32 (1998) 726.
[9] J. Wist, J. Sanabria, C. DieRolf, et al., J. Photochem. Photobiol. A 147 (2002) 241.
[10] A.G. Rincon, C. Pulgarin, N. Adler, J. Photochem. Photobiol. A 139 (2001) 233.
[11] S. Parra, S. Malato, C. Pulgarin, Appl. Catal. B: Environ. 36 (2002) 131.
[12] C. Pulgarin, S. Parra, M. Invernizzi, Catal. Today 62 (2000) 131.
[13] L. Sun, J.R. Bolton, J. Phys. Chem. 100 (1996) 4127.
[14] T.A. Egerton, C.J. King, J. Oil Col. Chem. Assoc. 26 (1979) 386.
[15] L. Belhacova, J. Krysa, J. Geryk, J. Jirkovsky, J. Chem. Technol. Biotechnol. 74 (1999) 149.
[16] Y.S. Choi, J.C. Lee, B.W. Kim, Korean J. Chem. Eng. 17 (2000) 633.
[17] C. Wei, W.Y. Lin, Z. Zainal, N.E. Williams, K. Zhu, A.P. Kruzic, R.L. Smith, K. Rajeshwar, Environ. Sci. Technol. 28 (1994) 934.

[18] Y.S. Choi, B.W. Kim, J. Chem. Technol. Biotechnol. 75 (2000) 1145.
[19] I.M. Butterfield, P.A. Christensen, A. Hamnett, K.E. Shaw, G.M. Walker, S.A. Walker, C.R. Howarth, J. Appl. Electrochem. 27 (1997) 385.
[20] I.M. Butterfield, P.A. Christensen, T.P. Curtis, J. Gunlazuardi, Water Res. 31 (1997) 675.
[21] P.A. Christensen, T.P. Curtis, B. Place, G.M. Walker, Water Res. 36 (2002) 2410.
[22] J.C. Harper, P.A. Christensen, T.A. Egerton, T.P. Curtis, J. Gunlazuardi, J. Appl. Electrochem. 31 (2001) 623.
[23] J.C. Harper, P.A. Christensen, T.A. Egerton, K. Scott, J. Appl. Electrochem. 31 (2001) 267.
[24] B. O'Regan, J. Moser, M. Anderson, M. Gratzel, J. Phys. Chem. 94 (1990) 8720.
[25] A. Hamnett, Compr. Chem. Kinetics 27 (1987) 61.
[26] K. Vinodgopal, U. Stafford, K.A. Gray, P.V. Kamat, J. Phys. Chem. 98 (1994) 6797.
[27] M. Ulmann, J. Augustynski, Chem. Phys. Lett. 141 (1987) 154.
[28] O.A. Semenikhin, V.E. Kazarinov, L. Jiang, K. Hashimoto, A. Fujishima, Langmuir 15 (1999) 3731.
[29] R. Flaig-Baumann, M. Hermann, H.P. Boehm, Z. Anorg. Allg. Chem. 372 (1970) 296.
[30] J. Criado, C. Real, J. Chem. Soc., Faraday Trans. 1 79 (1983) 2765.
[31] M. Abdullah, G.K.-C. Low, R.W. Matthews, J. Phys. Chem. 94 (1990) 6820.
[32] P.A. Christensen, T.A. Egerton, J.R. Tinlin, unpublished work.
[33] C.Y. Wang, J. Rabani, D.W. Bahnemann, J.K. Dohrmann, J. Photochem. Photobiol. A 148 (2002) 169.